Analyst

Cite this: DOI: 10.1039/c3an01169k

www.rsc.org/

Supplementary

Combined *in-situ* atomic force microscopy and infrared attenuated total reflection spectroelectrochemistry

Daniel Neubauer,[a] Jochen Scharpf,[b] Alberto Pasquarelli,[b] Boris Mizaikoff,[a] Christine Kranz,*[a]

Received 13th June 2013, Accepted 9th September 2013
DOI: 10.1039/c3an01169k

1. Characterization of the BDD-coated diamond ATR-electrode

The flat top part of the diamond ATR hemisphere was characterized by AFM before and after BDD coating (deflection images are presented in Figure S-1 A and B). In contrast to the present surface of the electrode, micro- or nanocrystalline BDD growth would be clearly evident due to different orientation of the crystal seeds, and therefore, different orientation of the resulting larger diamond crystallites.[1] While the polishing lines appear somehow smoothened in the AFM image after BDD deposition (Figure S-1 B), the grooves are still similar in depth (approximately 2 nm). Different orientation of the polishing lines merely originates from different alignment of the crystal in the AFM sample plate during AFM imaging. Changes in the optical and electrochemical properties of the diamond hemisphere were investigated along the fabrication process. High doping levels of boron within the deposited films are a prerequisite for sufficient conductivity. The reduction of infrared transparency due to boron doping over a broad spectral region was described in several publications[2–4], and was accounted for depositing thin films of BDD and a plasma etching step to remove excessive depositions from the sidewalls, which are directly within the infrared beam path.

During BDD growth, the sidewall of the crystal (i.e., incoupling location of the IR radiation) was not protected, and therefore, not only the top of the crystal but also the rounded sidewall was modified with a BDD layer. As IR radiation is coupled in at the sidewall of the crystal, the BDD layer significantly reduces the energy throughput. However, in contrast to the top surface of the ATR hemisphere, conductivity is only required at a small area of the crystal sidewall to establish electrical contact with the surface electrode. Consequently, an etching step was performed removing the BDD layer at approx. 75% of the sidewall area, thereby restoring approx. 30% of the initial infrared beam intensity (Figure S-1C). Further significant boron-induced absorption features were not observed in the IR energy spectrum (green), and hence, enable spectroelectrochemistry (SE) at the IR-transparent electrode.

[a] *Institute of Analytical and Bioanalytical Chemistry, University of Ulm, Albert-Einstein-Allee 11, 89081 Ulm, Germany. Fax: (+49)7315022463; Tel: (+49)7315022479; E-mail: christine.kranz@uni-ulm.de*
[b] *Institute of Electron Devices and Circuits, University of Ulm, Albert-Einstein-Allee 45, 89081 Ulm, Germany*

2. Generation of the analytical signal

Table 1 provides a summary of the different spatial dimensions, which are accessible by the individual analytical techniques of the combination. The BDD coating is not limited to the 400 x 400 µm flat crystal top; hence, the beveled surface area also contribute to the active electrode surface.

Technique	Probed surface area	Description
IR-ATR Spectroscopy	~ 0.16 mm^2	Octahedronal crystal top
Electrochemistry	~ 7 mm^2	Crystal top plus beveled sides
AFM measurements	max. 10x 10 µm or 100 x 100 µm	Determined by the available AFM scanner (Agilent)

Table S-1: Summary of the probed areas and geometric dimensions. These areas have to be considered when obtained data is interpreted.

3. Calculating the penetration depth of the evanescent field.

The penetration depth of the evanescent field can be calculated utilizing the following equation:[5]

$$d_p = \frac{\lambda}{2\pi\sqrt{n_1^2 \sin^2\theta - n_2^2}}$$

d_p = penetration depth, n_1 = refractive index (crystal), n_2 = refractive index (sample) $n_1 > n_2$, θ = angle of incidence (measured from surface normal) here 45°.

Please note that the intensity of the evanescent field exponentially decays with distance to the interface.

All calculations are based on previously published refractive index data for diamond[6], Ge[7], Si[7], ZnSe[8], and water[9]. The refractive index for every sample is certainly slightly different and in most cases the precise value is unknown. Therefore, water was considered as idealized sample. The lower the wavenumber, the higher is d_p Furthermore, crystal materials with a high refractive index (e.g., Ge) result in a lower d_p compared to diamond with a lower refractive index. Therefore, the application of diamond should provide a higher absorption signal, and thus, an improved signal-to-noise ratio.

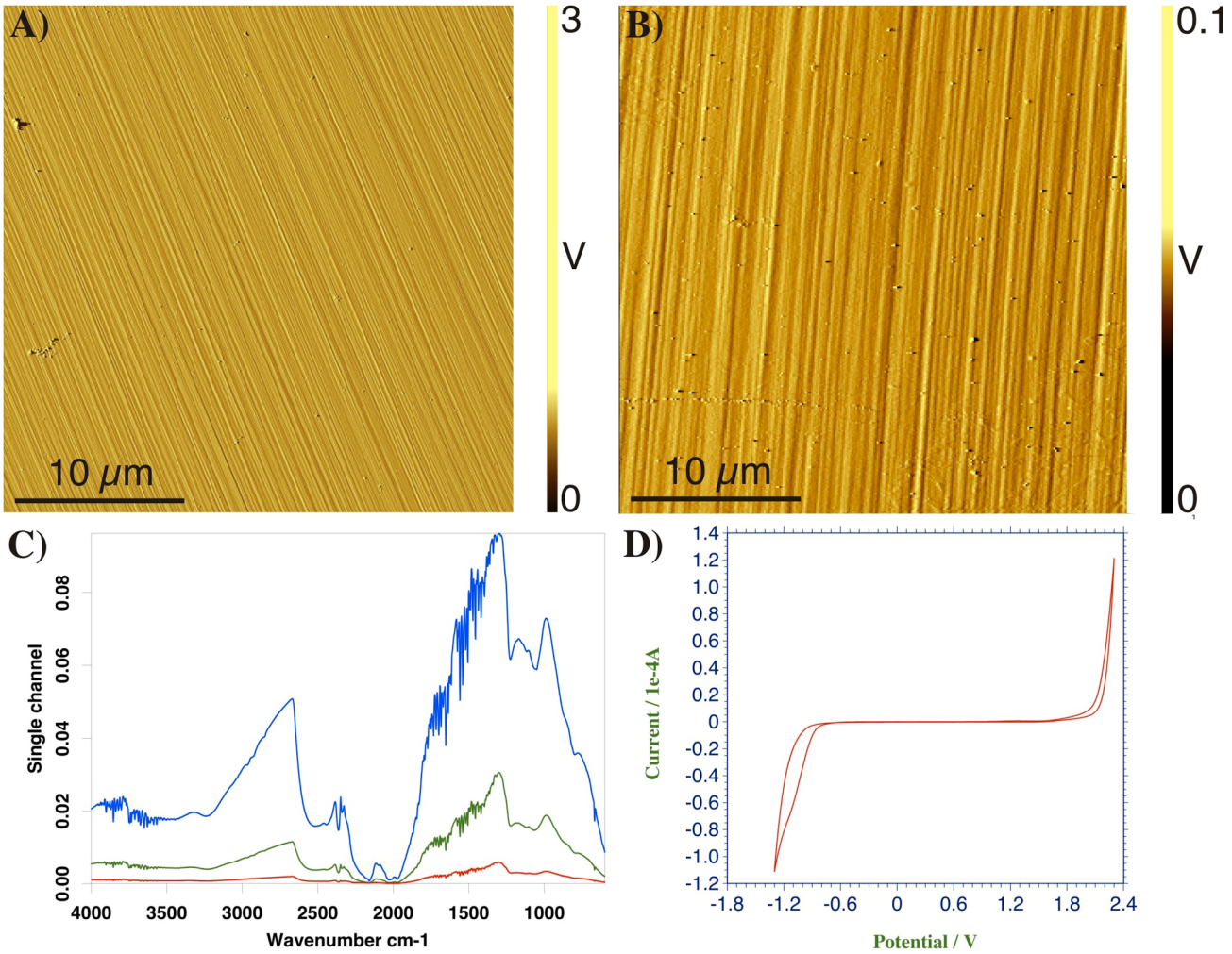

Figure S-1: A) AFM deflection image of the octahedonal ATR hemisphere before and B) after BDD coating. C) Infrared transmission (single beam energy) spectra of the diamond ATR hemisphere before BDD coating (blue), after BDD coating (red), and after the etching procedure (green). D) Exemplary cyclic voltammogram revealing the potential window of the BBD-modified ATR-crystal between 2.3 V and – 1.3 V vs. Ag/AgCl in 0.1 M H_2SO_4 (scan rate of 0.1 V/s; cycle starts at 0V positive direction).

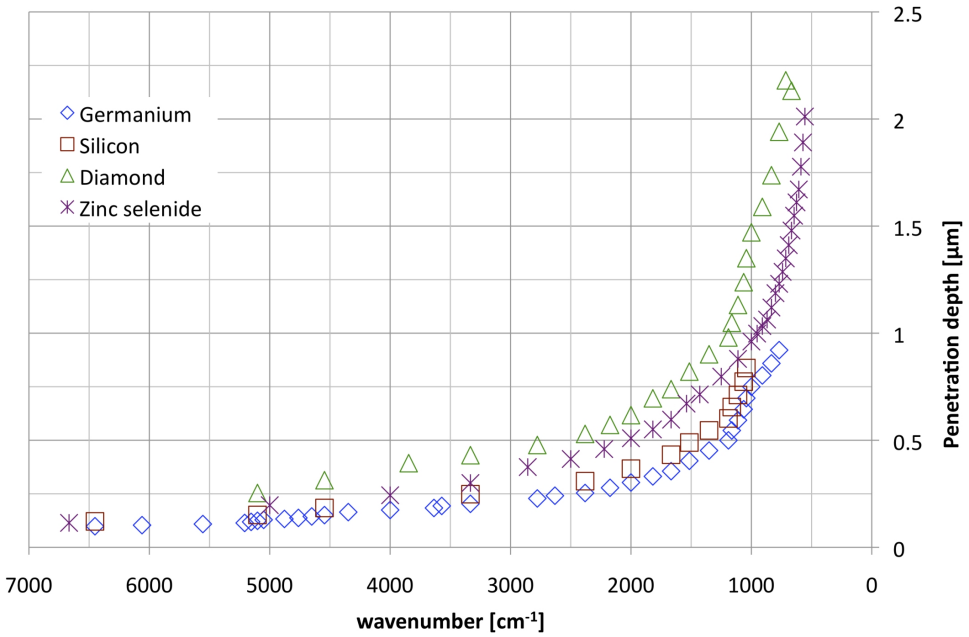

Figure S-2. Calculated penetration depth of the evanescent field vs. the wavenumber of incident radiation. The refractive index values are derived from literature.

Notes and references

1 S. Gupta, A. Dudipala, O. A. Williams, K. Haenen, and E. Bohannan, *J. Appl. Phys.*, 2008, **104**, 073514 1–12.
2 A. Deneuville, in *Semiconductors and Semimetals 76: Thin Film Diamond I*, eds. C. E. Nebel and J. Ristein, Elsevier B.V., Amsterdam, 1st edn., 2003, pp. 183–238.
3 R. Erz, W. Dötter, K. Jung, and H. Ehrhardt, *Diamond Relat. Mater.*, 1995, **4**, 469–472.
4 E. Bustarret, F. Pruvost, M. Bernard, C. Cytermann, and C. Uzan-Saguy, *Phys. Status Solidi A*, 2001, **186**, 303–307.
5 B. Mizaikoff, *Anal. Chem.*, 2003, **75**, 258 A–267 A.
6 D. F. Edwards and E. Ochoa, *J. Opt. Soc. Am.*, 1981, **71**, 607–608.
7 H. H. Li, *J. Phys. Chem. Ref. Data*, 1980, **9**, 561–658.
8 H. H. Li, *J. Phys. Chem. Ref. Data*, 1984, **13**, 103–150.
9 M. R. Querry, B. Curnutte, and D. Williams, *J. Opt. Soc. Am.*, 1969, **59**, 1299–1305.